scientific reports

Check for updates

OPEN

Deep eutectic solvent-supported poly(vinyl) alcohol electrospun anion-exchange membrane for potential application in alkaline fuel cells

Aida Barlybayeva, Bauyrzhan Myrzakhmetov, Yanwei Wang & Almagul Mentbayeva✉

This research introduces a new method to synthesize poly(vinyl) alcohol (PVA)-based deep eutectic solvent (DES)-supported anion-exchange membranes (AEMs) for alkaline fuel cell (AFC) applications. The fabrication method involved the modification of a PVA-based crosslinked nanofiber mat with DES prepared by mixing choline chloride (ChCl) and ethylene glycol (EG) in a 1:3 molar ratio. Various concentrations of glutaraldehyde (GA) solution were used to cross-link of the PVA fibers. The composite AEM developed using DES was designated as DES3@PVA4 and showed improved performance with a high hydroxide conductivity of 1.05 mS/cm at 60 °C, which is higher than that of the unmodified AEM (0.77 ± 0.01 mS/cm at 60 °C). The absence of swelling, enhanced elongation at break, and improved alkaline stability were further confirmed for the DES-modified AEM; the ionic conductivity remained stable after one month of soaking in 1 M potassium hydroxide solution. These results demonstrate that DES-enhanced PVA-based AEMs can be used for AFCs with improved conductivity, flexibility, mechanical strength, and alkaline stability compared to conventional AEMs.

Keywords Anion exchange membrane, Nanofibrous membrane, Ionic conductivity, Poly(vinyl) alcohol, DES

Due to the depletion of fossil fuel supplies and growing environmental concerns, there is a need for sustainable, economical, and environmentally friendly energy options. Fuel cells are a potential way to address these issues of all the existing alternative energy technologies[1].

Anion-exchange membrane fuel cells (AEMFCs) have recently gained significant research interest due to their advantages compared to well-investigated and commercialized proton-exchange membrane fuel cells (PEMFCs). Compared with platinum-based catalysts intended for PEMFCs, more affordable transition-metal catalysts can be used for the AEMFCs[2]. Other advantages include using a broad range of fuels, the excellent resistance to corrosion of widely applied cell material components in the alkaline medium, improved cell voltage, low fuel crossover, and faster oxygen reduction kinetics[3].

Anion-exchange membrane (AEM) is the crucial component of AEMFCs. It transports hydroxide ions from the cathode to the anode, acting as an ion conductor, gas barrier, and electron insulator[4]. It should satisfy the following requirements: sufficient conductivity of hydroxide ions, stability in alkaline solution at high temperatures, and exceptional mechanical and thermal stability during manufacturing and operation for the successful commercialization and widespread application of AEMFCs[5,6]. Despite the increasing research interest in AEMs, which have improved the functionality of membranes, they still have lower ionic conductivity and stability compared to Nafion membranes commonly used as a proton-exchange membrane (PEM), which delays their commercialization[7]. Thus, various modifications of AEM have been approached and investigated, along with choosing a suitable material.

To date, many researchers have developed quaternary ammonium (QA)-functionalized poly(vinyl) alcohol (PVA)-based AEMs for alkaline fuel cell (AFC) applications[8–10]. PVA, as the primary polymer backbone, has gained considerable interest due to its desirable properties, such as hydrophilicity associated with elevated water uptake, high ability to form fibers, and supposed to have higher ionic conductivity by functionalizing with QA groups[11]. However, QA group insertion is invariably not ecologically friendly, and the post-functionalization

Department of Chemical and Materials Engineering, School of Engineering and Digital Sciences, Nazarbayev University, Astana 010000, Kazakhstan. ✉email: almagul.mentbayeva@nu.edu.kz

approach obstructs the development of ion transport channels, which enhances ionic conductivity[12]. Furthermore, because of the cationic group degradation brought on by Hofmann elimination, ylide formation, and nucleophilic substitution, poor chemical stability in an alkaline medium and a high degree of swelling corresponding to low mechanical strength[13].

Various additives were investigated to address the drawbacks of QA groups in PVA-based AEMs for AFC application, such as cross-linkers[8–10], inorganic fillers[9,14], and ionic liquids (ILs)[12]. Introducing conductive and non-volatile ILs to AEMs may act as the "active sites" and speed up the conductivity of OH^- ions along with a cross-linking agent, improving mechanical stability[15,16]. Nevertheless, conventional ILs have a higher viscosity than water, leading to lower conductivity[17]. Moreover, the green character of ILs has often been challenged due to their relatively high toxicity and poor sustainability, requiring costly and complex preparation[18]. Deep eutectic solvents (DESs), the most promising type of ILs, prevail over conventional ILs due to low toxicity, straightforward preparation, and lower viscosity corresponding to higher ionic conductivity[17–19].

DES presents a typical model of the eutectic mixture, characterized by the hydrogen bonding between (or among) two compounds or more, such as hydrogen bond donors (HBDs) and hydrogen bond acceptors (HBAs), resulting in a new homogeneous compound with a decreased melting temperature[20,21]. Overall, modification with DES could enhance the properties of the membrane without affecting the structure of the polymer by an environmentally friendly and straightforward approach. In addition, QA salts as HBA consist of the above-mentioned QA groups, which could play the role of ion-functionalized charge groups and be attracted physically to the polymer backbone without quaternization, followed by a rise in ionic conductivity[12]. For example, choline chloride (ChCl) as HBA has QA groups, and in combination with ethylene glycol (EG) as HBD, they form DES through hydrogen bond interactions between the two components. The ChCl/EG DES remains in a liquid state, which promotes the ionic conductivity[22]. EG plays a role in reducing viscosity, thus facilitating improved ion transport and enhancing the overall ionic conductivity of the AEM[23].

According to Shahabi et al., one of their main contributions is the enhanced water movement that DESs provide after being integrated into membranes. Accordingly, DESs, in conjunction with water, could facilitate the transportation of hydroxide ions. However, due to DESs' sensitivity to high water content, their hydrogen bond interactions can be destroyed by water. Therefore, the absorption approach is the only viable method of doping them into the polymer matrix[24]. A suitable DES should, for this purpose, have the proper viscosity and affinity to be absorbed by the polymer matrix through straightforward immersion of the polymer in the DES[25].

So far, Rakhman et al. presented a work where a polymer electrolyte by impregnating PVA electrospun membrane with DES was developed and stated the potential of investigating this material for fuel cell application due to the improvement in electrical conductivity from 2.78×10^{-6} to 2.27×10^{-2} S/cm after immersion in DES[26]. Despite several articles that have studied ion exchange membranes, mainly for PEMs[17,25,27–29], to the best of our knowledge, research has not yet been conducted on the DES-supported AEM for AFC application. Furthermore, recently, DESs have become a viable substitute electrolyte for PEMFCs because of their unique characteristics and perspective advantages[25]. Thus, this work aims to show that the composition of the membrane indicated above is suitable for promoting the transport of hydroxide ions and highlighting the stability of the membrane in an alkaline medium.

To achieve this objective, a DES-supported crosslinked electrospun PVA-based AEM was developed. This involved fabricating a PVA-based nanofibrous mat using the electrospinning technique, subsequent cross-linking in glutaraldehyde solution, and modification through immersion in DES composed of choline chloride and ethylene glycol. The fabricated DES-supported PVA-based composite membranes with an average thickness of 100 μm demonstrated improved characteristics of alkali uptake, swelling ratio, ionic conductivity, chemical and mechanical stability, which can be considered for AFC applications.

Experimental

Material and methods

Polyvinyl alcohol (PVA, M_w 146,000–186,000, 87–89% hydrolyzed), glutaraldehyde (GA, 50 wt.% in H_2O), and ethylene glycol (EG, M_w 62.07 g/mol) were purchased from Sigma Aldrich. Choline chloride (ChCl, M_w 139.63 g/mol) was purchased from MP Biomedicals. All chemicals were of analytical grade and used as received without further purification.

PVA solution preparation and electrospinning

Figure 1 illustrates the fabrication procedure of DES-supported composite AEM. The PVA polymer-based nanofiber mat was fabricated using an electrospinning machine (Ne200 NanoSpinner, Inovenso, Turkey). The optimal concentration of PVA solution was chosen as 10 wt.% and was prepared at 80 °C for 12 h following the methods described in the literature[26,30,31]. 4.5 ml of PVA solution was injected into a 10 ml plastic syringe with a metallic nozzle tip and fed into the electrospinning machine. A drum collector wrapped in aluminum foil was used to collect fibers. The electrospinning parameters were optimized as follows: the flow rate was 0.8 ml/h, the distance between the nozzle tip and Al foil collector was 13 cm, and the high-voltage DC power supply was 19.5 kV. After obtaining the fibers, they were dried in a vacuum oven at 60 °C for 12 h.

Cross-linking

The pristine PVA fibers were crosslinked by immersing them in a solution prepared by dissolving GA (50 wt.% in H_2O) in ethanol, varying in concentration to 4, 6, and 8 wt.% for two days at room temperature. The pH was adjusted to 3 by adding 0.1 M hydrochloric acid. Afterward, the crosslinked membranes were washed with DI water to remove excess GA and dried for 12 h at 60 °C in a vacuum oven.

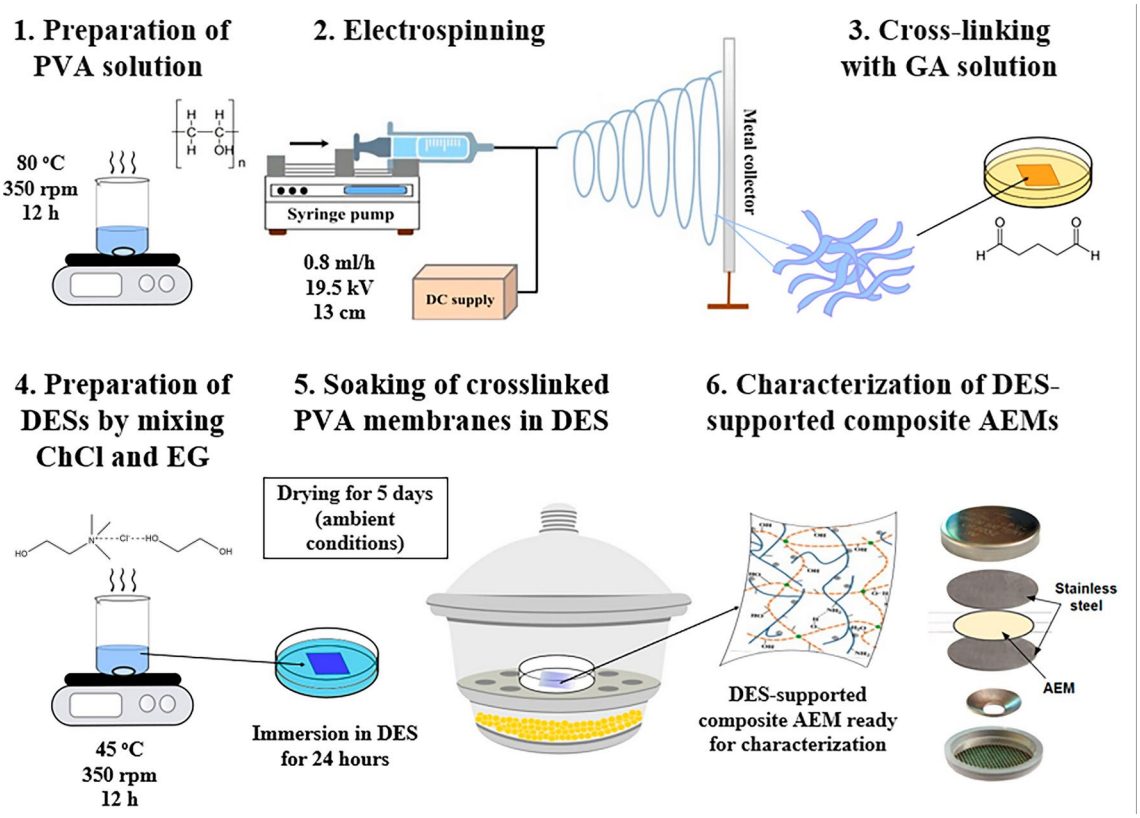

Fig. 1. Schematic representation of DES-supported composite AEM's fabrication.

Preparation of DES-supported PVA-based composite membranes

DESs were prepared according to procedures elsewhere[26,30]. To synthesize DESs, ChCl and EG were mixed at 45 °C for 12 h in four molar ratios: 1:1, 1:2, 1:3, and 1:4, respectively. Crosslinked PVA membranes were immersed into DES for 24 h and left in a desiccator to dry thoroughly for 5 days and characterized.

Characterization

To verify the accuracy of the data, triplicates of each type of AEMs were tested for each test.

Physical and chemical properties

Functional groups in the membranes and the interactions between various constituents were observed using Fourier transform infrared spectroscopy (FTIR, Thermo Fisher Scientific Nicolet iS10 FT-IR Spectrometer, USA). A transmission mode with a wavenumber range of 4000–500 cm^{-1} and 32 scans per sample were used. The surface morphology and structure of the obtained AEMs were examined by scanning electron microscopy (SEM, EDX ZEISS Crossbeam 540, Germany). The SEM samples were previously coated with gold using an automatic sputter coater (Q150T, Japan). Thermogravimetric analysis (TGA, STA 6000, Perkin Elmer, USA) was used to evaluate the thermal stability of the dried AEMs. Measurements were performed at a rate of 10 °C min^{-1} under an inert (dry nitrogen) atmosphere at 30–650 °C. The CHNS elemental analyzer (Elemental Vario micro cube, Germany) was used for elemental analysis at 1147 °C, with oxygen and helium flowing at 20 ml/min and 180 ml/min, respectively, to detect the DES-derived nitrogen content in the obtained AEMs. X-ray diffraction analysis (XRD, Rigaku MiniFlex 600 X-ray diffractometer, Japan) was performed to examine the phase composition of the AEMs with the following parameters: tube voltage of 40 kV, X-ray tube current of 15 mA, goniometer step size of 0.01° 2θ, and point intensity measurement time of 0.12 s.

Alkali uptake and swelling ratio

The AEMs were cut with a disc-punching machine to obtain a circular shape (d = 19 mm). The weight (m_{dry}) and diameter (d_{dry}) of the AEMs were measured, and after immersion for 24 h in a 1 M potassium hydroxide (KOH) solution and rinsing with DI water under ambient conditions. Alkali uptake and swelling ratio of DES-supported AEMs were determined using Eqs. (1) and (2), respectively[32,33]:

$$Alkaliuptake = \frac{m_{wet} - m_{dry}}{m_{dry}} \times 100\% \quad (1)$$

$$Swellingratio = \frac{d_{wet} - d_{dry}}{d_{dry}} \times 100\% \quad (2)$$

where m_{wet} and d_{wet} are weight and diameter of the wet membrane, while m_{dry} and d_{dry} refer to the weight and diameter of the dried membrane, respectively.

Ionic conductivity

Electrochemical impedance spectroscopy (EIS) (Metrohm Autolab, USA) was used to determine the ionic conductivity of fully hydrated AEMs at a 10^6 to 1 Hz frequency and a current of 100 mA. The measurements were performed at different temperatures between 25 and 60 °C. The ionic conductivity was measured within a certain time to investigate the alkaline stability. Before the conductivity test, the AEMs in the form of spherical discs (d = 19 mm) were placed in a 1 M KOH solution for 24 h and rinsed with DI water to remove potassium carbonates. The AEMs were placed between two stainless steel (SS) blocking electrodes in a coin-type cell for the test. The obtained Nyquist plots (see Supplementary Information, Fig. S1) were used to evaluate the bulk resistivity (R) of the membranes and calculate the ionic conductivity according to the Eq. (3) [34]:

$$\sigma = \frac{h}{RxS} \quad (3)$$

where, σ is the ionic conductivity (mS/cm), h is the thickness of the membrane (cm), R is the bulk resistivity of the membrane (Ω), and S is the cross-sectional area of the membrane (cm^2), $S = \frac{\pi \times d^2}{4}$.

Mechanical properties

Tensile test measurements were conducted using electronic universal testing equipment (WDW-3 Jinan HST Group Co., China) to examine the mechanical characteristics of the obtained AEMs. All the membranes were selected with similar dimensions, immersed in a 1 M KOH solution for 24 h, and rinsed with DI water. AEMs were cut into 20 × 50 mm pieces with a 20 mm gap between clampings and an elongation rate of 10 mm/min.

Results and discussion

Due to their high hydrophilicity, pristine PVA fibers were crosslinked with GA solutions of different concentrations, ranging from 4, 6, and 8 wt.%, designated PVA4, PVA6, and PVA8, respectively. As a result, the crosslinked PVA membranes remained stable in alkaline solution.

Among the other molar ratios DES3 (molar ratio of 1:3 ChCl to EG) was preferred as an additive. Compared with DES1 (molar ratio of 1:1 ChCl to EG) and DES2 (molar ratio of 1:2 ChCl to EG), DES3 showed higher homogeneity and transparency, which could better improve ionic conductivity due to its lower viscosity (see Supplementary Information; Fig. S2). DES4 (molar ratio of 1:4 ChCl to EG) was not considered, as DES3 was sufficient alternative to the most studied DES2[35,36]. In addition, the FTIR results for DESs showed the presence of functional groups originating from both ChCl and EG without the appearance of new peaks (see Supplementary Information; Fig. S3). DES3 was designated as DES for further results.

Accordingly, the obtained DES-supported composite AEMs were designated DES@PVA4, DES@PVA6, and DES@PVA8, respectively.

FTIR spectroscopy analysis of pristine and composite membranes

FTIR spectra of crosslinked PVA membrane, DES-supported AEM, and after their immersion in 1 M KOH solution for 24 h are shown in Fig. 2. According to the pristine PVA spectrum, the broad and strong peak at 3317 cm^{-1} corresponds to hydroxyl group OH^- within the PVA molecule, while the peak at 2916 cm^{-1} is attributed to the stretching of CH_2 on alkyl groups[37]. In addition, the intensive peaks at 1724 cm^{-1} and 1249 cm^{-1} are related to the C=O and C–O–C stretching from the PVA backbone[38] (Fig. 2A).

The PVA4-PVA8 spectra showed no difference and revealed a characteristic peak for C=O stretching from GA with a lower intensity at 1653 cm^{-1}, which is not visible in the pristine PVA spectrum[39] (see Supplementary Information; Fig. S4A). The appearance of this peak is supposed to show that cross-linking occurred within PVA. Since there is no significant difference among the spectra of PVA4–PVA8, the membrane with the lowest cross-linking degree, PVA4, was chosen to be immersed in KOH solution for 24 h and analyzed by FTIR. In the spectrum of PVA4/KOH (24 h), the disappearance of peaks at 1724 cm^{-1} and 1249 cm^{-1} was observed due to hydrolysis of the non-reacted acetyl groups from pristine PVA[38] (Fig. 2A). Moreover, the C=O peak at 1653 cm^{-1} from GA was preserved due to cross-linking.

Analogous to crosslinked PVA membranes, the spectra for the composite ones (DES@PVA4-DES@PVA8) show no differences (see Supplementary Information, Fig. S4B). Further, only the spectrum of DES@PVA4 was discussed. The spectrum of DES@PVA4 exhibits the carbonyl stretching frequency of C=O at 1724 cm^{-1} of PVA[38] (Fig. 2B). The presence of DES in the composite membranes was accompanied by two visible peaks, the asymmetric and symmetric CH_2 stretching at 2937 and 2869 cm^{-1}, respectively, originating from EG. In addition, a peak at 953 cm^{-1} NR_4^+ stretching of the QA group was observed, originating from ChCl, where R = CH_3[40]. The introduction of DES led to noticeable changes in the peak at 1481 cm^{-1}, corresponding to the CH_2 bending most evident in all ChCl-based DES[41]. Nevertheless, the intensity of DES@PVA4/KOH spectrum (24 h) decreased after immersion in KOH solution due to the presumed leaching of DES.

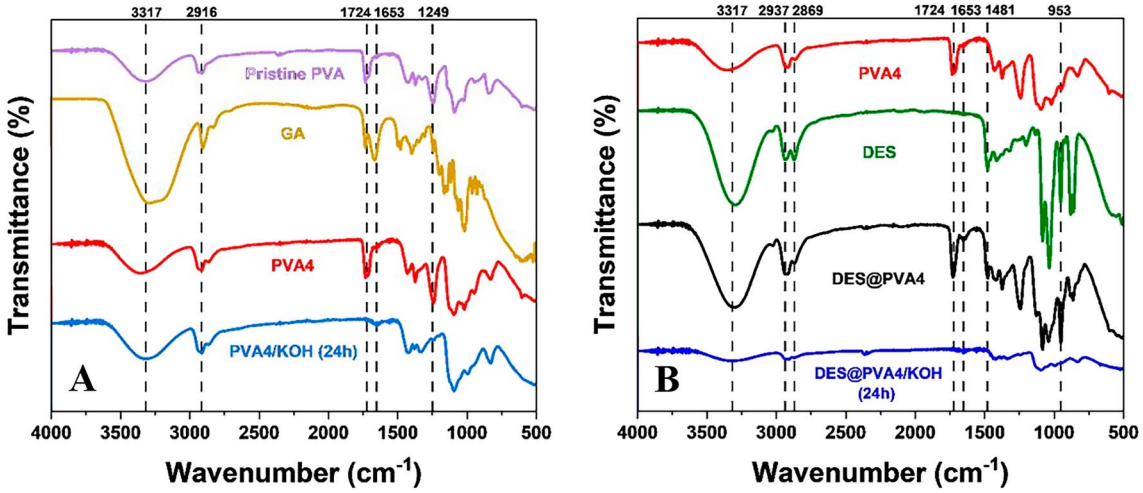

Fig. 2. FTIR spectra for: (**A**) pristine PVA, GA, PVA4, PVA4/KOH (24 h) and (**B**) PVA4, DES, DES@PVA4, and DES@PVA4/KOH (24 h).

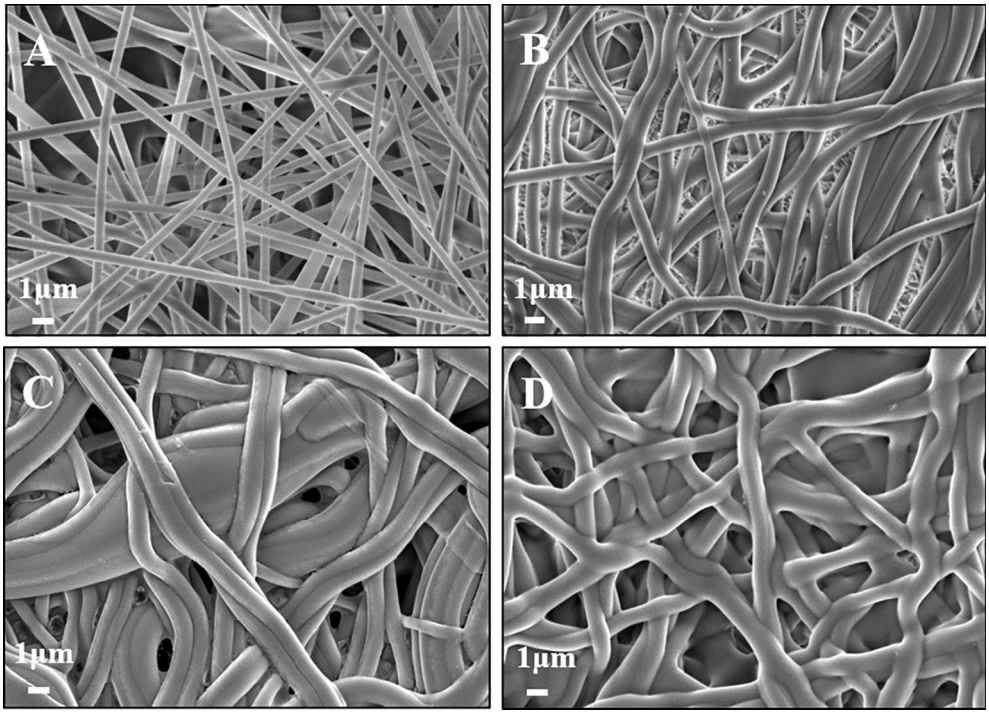

Fig. 3. SEM images of (**A**) pristine PVA, (**B**) PVA4, (**C**) DES@PVA4, and (**D**) DES@PVA4/KOH (24 h).

Based on the FTIR results, the functional groups of PVA and DES in the DES-supported AEM composite were compared; no new peak was identified in the spectra. Therefore, DES is assumed to be physically absorbed in the PVA membrane due to hydrogen bonding interactions and does not react chemically with PVA.

Surface characterization of pristine and composite membranes

SEM was used to analyze the surface morphology of pristine PVA, PVA4, and DES@PVA4 membranes before and after immersion in a 1 M KOH solution, as illustrated in Fig. 3.

Pristine PVA fibers have a uniform diameter distribution of 400–500 nm (Fig. 3A). The morphology of pristine PVA fibers is smooth without beads or entanglements. Cross-linking of PVA fibers with GA solution resulted in a more robust and rigid material with a denser structure in accordance with the literature[31]. In the membranes formed after cross-linking, the fibers changed their shape from straight to relaxed, slightly enlarged in diameter around 1.5 times (700–800 nm), and merged as entanglements in some areas (Fig. 3B). Thus, there is a clear difference between the SEM images of pristine PVA and the crosslinked PVA. In addition, the PVA

fibers overlap and form a three-dimensional networked area with the voids, where DES could be occupied[26]. The membranes with PVA6 and PVA8 have very similar surface morphology with PVA4 (see Supplementary Information, Fig. S5).

DES was introduced into this system by simply immersing the crosslinked PVA membrane, resulting in DES-supported composite AEM. As can be seen from Fig. 3C, the uptake of DES resulted in relaxed fibers with adherence to each other, shape change, and increase in diameter (850–1200 nm). Ion conduction is thought to be maintained by the liquid phase of the DES in the voids and the fibers. To check its stability, AEM was also immersed in KOH solution for 24 h. As can be seen in Fig. 3D, the fibers within almost the same diameter remained relaxed, but less adherence between them was observed.

TGA and CHNS analysis of pristine and composite membranes

TGA and CHNS analysis can be used to qualitatively and quantitatively confirm the presence of DES in the composite membranes by examining the variation of the weight loss curves and quantitatively determining the nitrogen content from ChCl, respectively. Figure 4 shows the results obtained with these two methods.

In Fig. 4A, the initial weight loss of the pristine PVA fibers around 100 °C is due to the evaporation of the absorbed water molecules. The second weight loss, which occurred in a temperature range of 250–370 °C, was caused by the initial degradation of the PVA backbone. The third weight loss, which occurred at 390–475 °C, is related to the degradation of the vinyl acetate group[8,9,42]. The central part of the weight loss of the pristine PVA fibers occurred at about 325 °C. At the thermogravimetric curves of the crosslinked membranes (PVA4-PVA8), the degradation of GA occurs between 150 and 305 °C. The subsequent weight loss above 305 °C was associated with the degradation of PVA itself[9]. Crosslinked PVA membranes showed improved thermal stability compared to pristine PVA fibers[42]. The thermogravimetric curves of all composite membranes included two levels of weight loss, from 100 to 200 °C and 200–300 °C, matching EG and ChCl, respectively[43]. The weight loss curve started at around 250 °C, indicating the thermal degradation of PVA[30].

Based on the TGA results, a significant difference between pristine PVA and DES-supported AEMs was observed. Each weight loss region of the DES-supported AEMs' curve qualitatively indicated the presence of the main components, starting with the evaporation of EG and the degradation of ChCl and then PVA, respectively. Moreover, all DES-supported AEMs are thermally stable within the operational temperature of AFCs[44].

Figure 4B shows the carbon, hydrogen, and nitrogen content of pristine PVA and DES-supported composite membranes. As expected, untreated PVA membranes contained carbon and hydrogen only, while the DES-supported composite AEM had a nitrogen content of 3.16 ± 0.05 wt.%, confirming the presence of DES in the membrane.

Alkali uptake and swelling ratio of crosslinked and composite membranes

1 M KOH solution was chosen as the conductive aqueous medium to study the uptake and swelling of the prepared membranes[33,45]. As one of the main components, water must be present in AEMs to achieve high OH^- conductivity[1]. Water clusters can increase ionic conductivity, which acts as anion transport pathways within the AEM. On the other hand, significant swelling of the membrane by KOH solution could be due to excessive alkali uptake. This could lead to poor dimensional stability and affect the ion-conducting performance of the membrane[1]. So, alkali uptake balancing within AEM is needed. Figure 5 illustrates how the modification with DES affected the alkali uptake of the composite AEMs compared to non-modified ones.

Modification with DES as an additive for crosslinked PVA membranes led to increased hydrophilicity. Consequently, the alkali uptake ability increased from 270 ± 4% (unmodified with DES AEM, PVA4) to 364 ± 4% (modified AEM, DES@PVA4). At the same time, the alkali uptake of DES@PVA decreased with the increase of GA concentration, resulting in alkali uptake values of 310 ± 2% (DES@PVA6) and 306 ± 3% (DES@

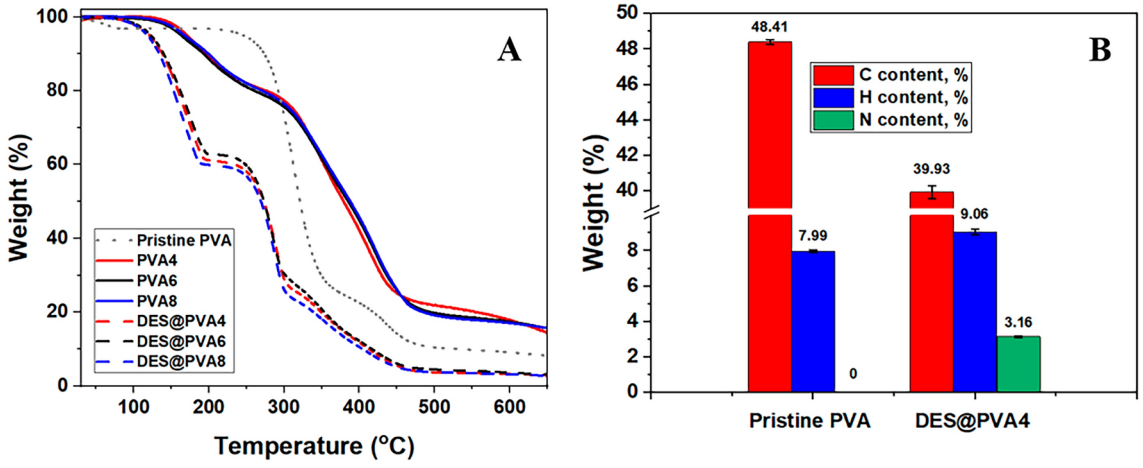

Fig. 4. (**A**) Thermogravimetric curves of pristine PVA, PVA4-8, DES@PVA4-8 and (**B**) carbon, hydrogen, and nitrogen content charts of pristine PVA, DES@PVA4.

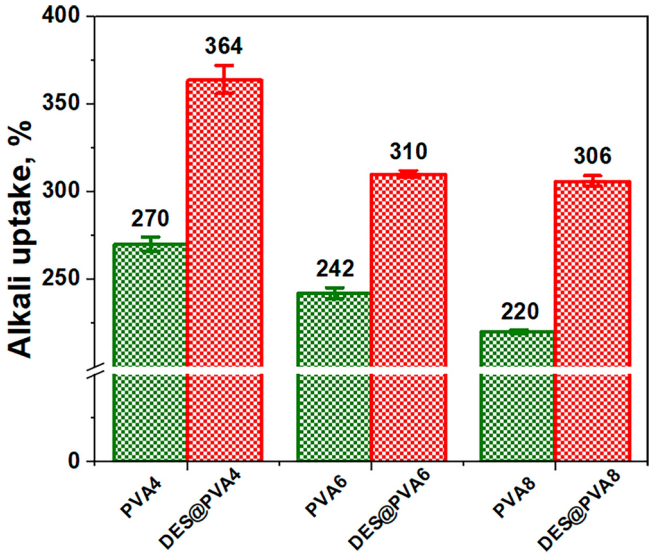

Fig. 5. Alkali uptake charts of PVA4-8 and DES@PVA4-8.

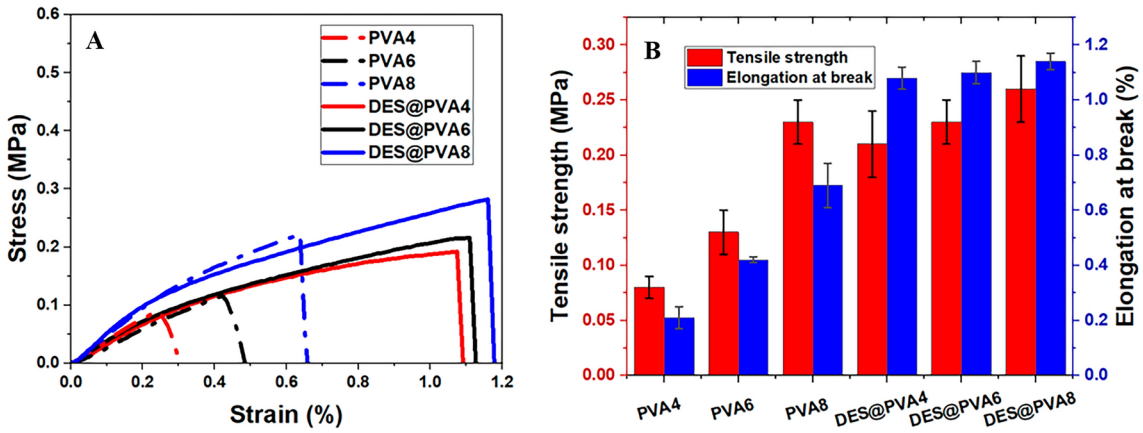

Fig. 6. (**A**) Stress–strain curves and (**B**) tensile strength-elongation at break charts of crosslinked PVA membranes and DES-supported composite AEMs.

PVA8), respectively. The results for the alkali uptake of the unmodified crosslinked membranes also showed the same trend (Fig. 5). The increase in cross-linking degree resulted in a denser and more compact micro-network structure, which was accompanied by a restricted space for ion transport, which was the main cause of the reduction in alkali uptake[1,46].

It is expected that the significant hygroscopicity of DES can lead to an increase in alkali uptake and swelling ratio due to the hydrophilic groups Cl^- and OH^- present in the molecule[47]. Swelling ratio was measured by the change in diameters of the dry and wet states of the membrane. Nevertheless, no difference was observed in all membranes' lateral dimensions, regardless of the large value of alkali uptake. It might be due to the highly porous nanofiber structure resulting in the trapping of alkaline solution in the voids[43]. Swelling of the crosslinked fibers is facilitated by the presence of voids within the structure.

Overall, the modification with DES and the PVA hydrophilicity indicates that the nanofiber structure absorbed the alkaline solution (each fiber swelled up). AEMs are believed to have higher ionic conductivities while suppressing dimensional changes. Therefore, swelling ratio was equal to zero, resulting in high dimensional stability and mechanical properties[48].

Mechanical properties of crosslinked and DES-supported composite membranes

The assembly of the cell requires careful consideration of the mechanical properties, such as tensile strength and elongation at break of the AEMs[9]. Accordingly, the mechanical stability of the crosslinked PVA- and DES-supported composite AEMs after immersion in 1 M KOH solution and rinsing with DI water was investigated using the stress–strain curves and tensile strength-elongation at break bar graphs shown in Fig. 6.

An improvement in mechanical properties was observed with the increase of the cross-linking degree of unmodified PVA membranes. It is assumed that cross-linking reduces the deformation of the membranes, which can lead to a loss of elasticity and increased brittleness[43]. The PVA4 with the lowest cross-linking degree had the greatest alkali uptake and was supposed to be mechanically weaker. The tensile strength and elongation at break of PVA4 were 0.08 ± 0.01 MPa and $0.21 \pm 0.04\%$, respectively (Fig. 6). When the concentration of GA solution was changed from 4 to 8 wt.%, the tensile strength and elongation at break were increased by 2.9 and 3.3 times, respectively. The same trend was observed with the increase in the degree of cross-linking for the modified AEMs. The variation of tensile strength and elongation at break was insignificant, and the values were practically the same. However, introducing DES into the system led to a noticeable improvement in mechanical properties, especially elongation. Accordingly, the tensile strength and elongation at break of DES@PVA4 were 0.21 ± 0.03 MPa and $1.08 \pm 0.04\%$, respectively. Thus, the elongation at break of DES@PVA4 was almost 5.1 times higher than that of unmodified crosslinked PVA membranes. DES@PVA8 exhibited the highest tensile strength of 0.26 ± 0.03 MPa and an elongation at break of $1.14 \pm 0.03\%$.

The results show that strong interactions between the polymer matrix and DES lead to improved mechanical properties. The introduced DES most likely strengthened the amorphous phases of the polymer matrix, which may reduce its crystallinity[28,49]. Moreover, XRD spectra showed that after introducing DES into the PVA matrix, the intensity of the peak decreased, which means that the crystallinity of the composite membrane reduced compared to the crosslinked one (see Supplementary Information, Fig. S6). Also, the presence of DES likely enhances hydrogen bonding and van der Waals interactions within the PVA-DES system, leading to a plasticizing effect, as suggested by the increased elongation at break.

Ionic conductivity of crosslinked and composite membranes

Ion exchange capacity (IEC) is a crucial parameter for ion-exchange membranes, reflecting their ability to exchange ions, typically through covalently bonded ionic groups in the polymer matrix[50]. As mentioned above, many studies have applied IEC to test PVA-based quaternized AEMs[8–10]. However, for the DES-supported AEMs, the QA groups from ChCl are only physically attracted to the polymer matrix via van der Waals forces, as quaternization was not performed[12]. Therefore, IEC analysis does not apply to this system. Instead, ionic conductivity was examined using EIS, which is more appropriate for systems where the ionic species are not chemically bonded but exhibit physical interactions.

All DES-supported composite membranes with different degrees of cross-linking and a thickness of about 100 μm were tested by EIS to investigate ionic conductivity at temperatures from 25 to 60 °C, which is a practical condition for the operation of alkaline fuel cells with AEMs[51]. Before assembling the cell, the membranes were immersed in a 1 M KOH solution for 24 h, and the membrane surface was lightly rinsed with DI water. In DESs, the number of available carriers and the viscosity of the ion-conducting medium are the most important parameters that determine the ionic conductivity of the solutions. In the ChCl/EG-based DES used in this work, the positively charged QA groups are the main charge carriers. In addition, the extent of hydrogen bonding between the HBA and the HBD determines the viscosity of the solution[52]. Due to their relatively high viscosity, most DESs have a low ionic conductivity due to their composition.

Figure 7A-B shows and compares the dependence of ionic conductivity of unmodified crosslinked membranes and DES-supported composite AEMs on temperature. In addition, the alkaline stability over different periods (Fig. 7C) was studied. As expected, the ionic conductivity of the individual AEM composites increased with temperature under the same conditions, as the ion mobility rose and the viscosity of the DES decreased at higher temperatures[1,53,54] (Fig. 7A,B). In addition, higher temperatures could cause the free space of the AEMs to expand, which is beneficial for ion conduction[1]. For all modified composite AEMs, the ionic conductivity varied between 0.5 and 1.1 mS/cm at lower and higher temperatures (Fig. 7A). The ionic conductivity and alkali uptake showed the same trend (Fig. 5).

It is also noteworthy that the cross-linking agent serves an important additional role in the PVA/DES structure. With the increase in the concentration of GA from 4 to 8 wt.%, a decrease in ionic conductivity was observed due to the higher degree of cross-linking. Thus, increasing the degree of cross-linking improved the mechanical properties of the membrane but decreased the water and DES absorption, leading to a lack of OH^- groups in the system[43]. Since DES@PVA4 exhibited the highest values of ionic conductivity, such as 0.66 ± 0.03 mS/cm at room temperature, 1.01 ± 0.01 mS/cm at 40 °C, and 1.05 ± 0.02 mS/cm at 60 °C (Fig. 7A), DES@PVA4 was compared with the unmodified PVA4 to evaluate the effect of DES on ionic conductivity.

Figure 7B shows that DES increased the hydroxide conductivity of DES@PVA4 compared to unmodified PVA4. After the introduction of DES into the PVA fibers, the ionic conductivity raised from 0.56 ± 0.07 to 0.66 ± 0.03 mS/cm at room temperature, and the same trend was observed for higher temperatures reaching 1.05 ± 0.02 mS/cm at 60 °C. A significant difference between the ionic conductivity values is observed when the temperature is increased from 25 to 40 °C (Fig. 7A,B). However, there was a slight increase in ionic conductivity from 40 to 60 °C. This could be related to the onset of evaporation of water from the alkaline solution in this temperature range. DES@PVA4 thus proved to be the AEM with the highest ionic conductivity and good mechanical properties due to a higher degree of elongation than the original PVA membranes.

Alkaline stability of crosslinked and DES-supported composite membranes

The membranes' alkaline stability was tested by immersing them in a 1 M KOH solution for different periods and monitoring their ionic conductivity. As shown in Fig. 7C, increasing the OH^- ion and H_2O content on day 3 significantly improved the PVA/DES ionic conductivity[17]. From this result, it can be concluded that increasing the concentration of OH^- ions and H_2O led to an improvement in the ionic conductivity of DES[55]. It was also found that due to the low molecular weight of water, the hydroxyl groups of EG could not preferably interact with ChCl to form a highly viscous solution. This could be due to the decreased viscosity of aqueous DESs,

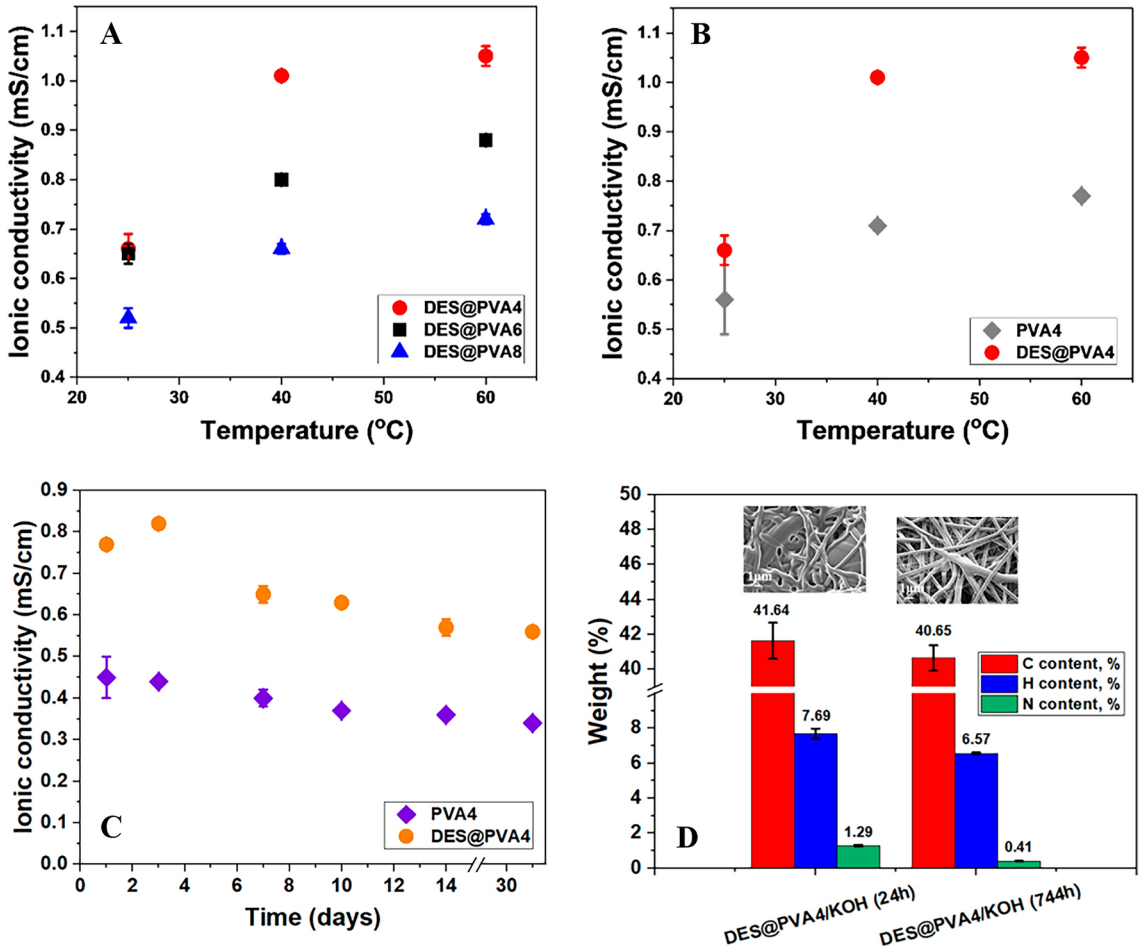

Fig. 7. Ionic conductivity at 25, 40, and 60 °C of (**A**) DES@PVA4-8, (**B**) PVA4, DES@PVA4, (**C**) alkaline stability of PVA4 and DES@PVA4 at different periods, and (**D**) carbon, hydrogen, and nitrogen content charts and SEM images of DES@PVA4/KOH (24 h), DES@PVA4/KOH (744 h).

which may have increased ionic conductivity. However, it might be concluded that the presence of water reduced the interactions between HBD and HBA, which had only a minor effect on the physicochemical properties of the DES on day 7. This finding suggests that adding water slightly altered the interaction dynamics within the DES and its properties over time. No fluctuations in ionic conductivity were observed throughout the 1-month immersion, implying that the physicochemical properties of the material remained consistent and unchanged during this time. This observation indicates that the OH^- ion and the water did not destabilize the hydrogen bond network but became part of it by forming new bonds. The preservation of the structure of the eutectic compound demonstrates the stability and mechanical strength of the DES-supported composite membrane after being exposed to the KOH solution for a prolonged period of time.

Furthermore, it was hypothesized that the long exposure time of the membrane in the KOH solution could have led to leaching, i.e. migration or release of DES components. However, it was observed that the DES was still firmly anchored in the membrane after the repeated washing steps, as confirmed by the characteristic CHNS data and the slight changes in thermal stability by TGA (Fig. 4A). As shown in Fig. 7D, the nitrogen content decreased to 1.29 ± 0.04 wt.% after 24 h of immersion in 1 M KOH solution. However, even after one month of immersion in an alkaline solution, the membranes' nitrogen content stayed at 0.41 ± 0.01 wt.%. SEM images (Fig. 7D) show the fibers are still relaxed and stable. The excess of DES was leached out when comparing 1-day and 1-month immersion of AEM in KOH solution. Nevertheless, the CHNS and alkaline stability results showed that a small amount of DES remained in the AEM, which can still improve or maintain the ionic conductivity of the membranes: the ionic conductivity of DES@PVA4 was 1.65 times higher than that of PVA4 after immersion in KOH for 1 month.

Conclusions

The development of electrospun PVA-based AEMs employing a new fabrication technique has shown promising results for application in AFC. Using DES as an additive combined with PVA fibers and crosslinked with various concentrations of GA has considerably improved membrane properties. The DES-supported composite AEMs with a thickness of 100 µm, particularly the DES3@PVA4 crosslinked with a 4 wt.% GA solution, exhibited a

better hydroxide ion conductivity of 1.05 mS/cm at 60 °C, surpassing the performance of unmodified AEMs (0.77 ± 0.01 mS/cm at 60 °C). The absence of swelling enhanced alkali uptake ($364 \pm 8\%$), improved elongation at break, and improved alkali stability, which underlines the advantages of DES-modified AEMs. Furthermore, the stable ionic conductivity, even after prolonged exposure to a 1 M potassium hydroxide solution, demonstrates the long-term durability and performance of DES-supported AEMs. These results position PVA-based DES-supported AEMs as promising candidates for AFC applications, as they offer higher hydroxide conductivity, flexibility, mechanical strength, and alkaline stability than conventional AEMs.

Data availability

All data supporting the research in this paper are available in the main text and Supplementary Information.

Received: 27 July 2024; Accepted: 21 October 2024
Published online: 27 October 2024

References

1. Samsudin, A. M. & Hacker, V. Preparation and characterization of PVA/PDDA/nano-zirconia composite anion exchange membranes for fuel cells. *Polymers.* **11**, 1399 (2019).
2. Hren, M., Božič, M., Fakin, D., Kleinschek, K. S. & Gorgieva, S. Alkaline membrane fuel cells: Anion exchange membranes and fuels. *Sustain Energy Fuels.* **5**, 604–637 (2021).
3. Iravaninia, M. & Rowshanzamir, S. Polysulfone-based anion exchange membranes for potential application in solid alkaline fuel cells. *J. Renew. Energy Environ.* **2**, 59–65 (2015).
4. Ran, J. et al. Ion exchange membranes: New developments and applications. *J. Membrane Sci.* **522**, 267–291 (2017).
5. Merle, G., Wessling, M. & Nijmeijer, K. Anion exchange membranes for alkaline fuel cells: A review. *J. Membrane Sci.* **377**, 1–35 (2011).
6. Ferriday, T. B. & Middleton, P. H. Alkaline fuel cell technology—A review. *Int. J. Hydrogen Energy.* **46**, 18489–18510 (2021).
7. Das, G., Choi, J.-H., Nguyen, P. K. T., Kim, D.-J. & Yoon, Y. S. Anion exchange membranes for fuel cell application: A review. *Polymers.* **14**, 1197 (2022).
8. Hari Gopi, K. & Bhat, S. D. Anion exchange membrane from polyvinyl alcohol functionalized with quaternary ammonium groups via alkyl spacers. *Ionics.* **24**, 1097–1109 (2018).
9. Samsudin, A. M., Roschger, M., Wolf, S. & Hacker, V. Preparation and characterization of QPVA/PDDA electrospun nanofiber anion exchange membranes for alkaline fuel cells. *Nanomaterials.* **12**, 3965 (2022).
10. Du, X., Zhang, H., Yuan, Y. & Wang, Z. Semi-interpenetrating network anion exchange membranes based on quaternized polyvinyl alcohol/poly(diallyldimethylammonium chloride). *Green Energy Environ.* **6**, 743–750 (2021).
11. Hsu, P.-Y. et al. Highly zeolite-loaded polyvinyl alcohol composite membranes for alkaline fuel-cell electrolytes. *Polymers.* **10**, 102 (2018).
12. Wang, D., Wang, Y., Wang, J. & Wang, L. Synthesized Geminal-imidazolium-type ionic liquids applying for PVA-FP/[DimL][OH] anion exchange membranes for fuel cells. *Polymer.* **170**, 31–42 (2019).
13. Couture, G., Alaaeddine, A., Boschet, F. & Ameduri, B. Polymeric materials as anion-exchange membranes for alkaline fuel cells. *Progress Polym. Sci.* **36**, 1521–1557 (2011).
14. Das, G., Deka, B. K., Lee, S. H., Park, Y.-B. & Yoon, Y. S. Poly(vinyl alcohol)/silica nanoparticles based anion-conducting nanocomposite membrane for fuel-cell applications. *Macromol. Res.* **23**, 256–264 (2015).
15. Chu, Y., Chen, Y., Chen, N., Wang, F. & Zhu, H. A new method for improving the ion conductivity of anion exchange membranes by using TiO_2 nanoparticles coated with ionic liquid. *RSC Adv.* **6**, 96768–96777 (2016).
16. Li, P., Li, K., Chen, J., Zhang, N. & Tang, S. Novel anion exchange membrane with poly ionic liquid-confined hypercrosslinked polymer for enhanced anion conduction and stability. *Int. J. Hydrogen Energy.* **46**, 21590–21599 (2021).
17. Karimi, M. B., Mohammadi, F. & Hooshyari, K. Non-humidified fuel cells using a deep eutectic solvent (DES) as the electrolyte within a polymer electrolyte membrane (PEM): The effect of water and counterions. *Phys. Chem. Chem. Phys.* **22**, 2917–2929 (2020).
18. Płotka-Wasylka, J., de la Guardia, M., Andruch, V. & Vilková, M. Deep eutectic solvents vs ionic liquids: Similarities and differences. *Microchem. J.* **159**, 105539 (2020).
19. Armandsefat, F., Hamzehzadeh, S. & Azizi, N. Efficient and promising oxidative desulfurization of fuel using Fenton like deep eutectic solvent. *Sci. Rep.* **14**, 12614 (2024).
20. Jiang, B. et al. Novel supported liquid membranes based on deep eutectic solvents for olefin-paraffin separation via facilitated transport. *J. Membrane Sci.* **536**, 123–132 (2017).
21. Phillips, J., Focke, W. W., du Toit, E. L. & Wesley-Smith, J. Deep eutectic solvents for solid pesticide dosage forms. *Sci. Rep.* **10**, 20729 (2020).
22. Hayler, H. J. & Perkin, S. The eutectic point in choline chloride and ethylene glycol mixtures. *Chem. Commun.* **58**, 12728–12731 (2022).
23. Tran, K. T. T. et al. New deep eutectic solvents based on ethylene glycol—LiTFSI and their application as an electrolyte in electrochemical double layer capacitor (EDLC). *J. Mol. Liq.* **320**, 114495 (2020).
24. Seyyed Shahabi, S., Azizi, N. & Vatanpour, V. Tuning thin-film composite reverse osmosis membranes using deep eutectic solvents and ionic liquids toward enhanced water permeation. *J. Membrane Sci.* **610**, 118267 (2020).
25. Karimi, M. B., Mohammadi, F. & Hooshyari, K. Potential use of deep eutectic solvents (DESs) to enhance anhydrous proton conductivity of Nafion 115® membrane for fuel cell applications. *J. Membrane Sci.* **611**, 118217 (2020).
26. Rahman, S. M. et al. Synthesis and characterization of polymer electrolyte using deep eutectic solvents and electrospun poly(vinyl alcohol) membrane. *Ind. Eng. Chem. Res.* **55**, 8341–8348 (2016).
27. Xu, J., Hao, J., Zhai, Y. & Wang, Y. Deep eutectic solvents based on N, N, N-trimethyl propylsulphonate ammonium hydrosulfate-urea as potential electrolytes for proton exchange membrane fuel cell. *J. Power Sources.* **580**, 233385 (2023).
28. Wong, C. Y. et al. Effect of deep eutectic solvent in proton conduction and thermal behaviour of chitosan-based membrane. *J. Mol. Liquids.* **269**, 675–683 (2018).
29. Karimi, M. B., Mohammadi, F. & Hooshyari, K. Effect of deep eutectic solvents hydrogen bond acceptor on the anhydrous proton conductivity of Nafion membrane for fuel cell applications. *J. Membrane Sci.* **605**, 118116 (2020).
30. Mano, F. et al. Production of poly(vinyl alcohol) (pva) fibers with encapsulated natural deep eutectic solvent (NADES) using electrospinning. *ACS Sustain Chem. Eng.* **3**, 2504–2509 (2015).
31. Hulupi, M. & Haryadi, H. Synthesis and characterization of electrospinning PVA nanofiber-crosslinked by glutaraldehyde. *Mater. Today Proc.* **13**, 199–204 (2019).
32. Hou, J. et al. Recyclable cross-linked anion exchange membrane for alkaline fuel cell application. *J. Power Sources.* **375**, 404–411 (2018).

33. Huang, C.-Y. et al. Alkaline direct ethanol fuel cell performance using alkali-impregnated polyvinyl alcohol/functionalized carbon nano-tube solid electrolytes. *J. Power Sources.* **303**, 267–277 (2016).
34. Jang, S., Chuang, F., Tsen, W. & Kuo, T. Quaternized chitosan/functionalized carbon nanotubes composite anion exchange membranes. *J. Appl. Polym. Sci.* **136** (2019).
35. Kazarina, O. V. et al. The role of HBA structure of deep eutectic solvents consisted of ethylene glycol and chlorides of a choline family for improving the ammonia capture performance. *J. Mol. Liquids.* **373**, 121216 (2023).
36. Usman, M. A., Fagoroye, O. K., Ajayi, T. O. & Kehinde, A. J. Ternary liquid–liquid equilibrium data for n-Hexane-Benzene-DES (choline chloride/ethylene glycol, choline chloride/glycerol, choline chloride/urea) at 303 K and 101.3 kPa. *Appl. Petrochem. Res.* **10**, 125–137 (2020).
37. Hong, X., He, J., Zou, L., Wang, Y. & Li, Y. V. Preparation and characterization of high strength and high modulus PVA fiber via dry-wet spinning with cross-linking of boric acid. *J. Appl. Polym. Sci.* **138**, (2021).
38. Velez, A. A. I. et al. Properties of the PVA-VAVTD KOH blend as a gel polymer electrolyte for zinc batteries. *Gels.* **7**, 256 (2021).
39. Matty, F. S., Sultan, M. T. & Amine, AKh. Swelling behavior of cross-link PVA with glutaraldehyde. *Ibn AL-Haitham J. Pure Appl. Sci.* **28**, 136–146 (2015).
40. Çabuk, H., Yılmaz, Y. & Yıldız, E. Vortex-assisted deep eutectic solvent-based liquid-liquid microextraction for the analysis of alkyl gallates in vegetable oils. *Acta Chimica Slovenica.* **66**, 385–394 (2019).
41. Delgado-Mellado, N. et al. Thermal stability of choline chloride deep eutectic solvents by TGA/FTIR-ATR analysis. *J. Mol. Liquids.* **260**, 37–43 (2018).
42. Kim, K.-O., Akada, Y., Kai, W., Kim, B.-S. & Kim, I.-S. Cells attachment property of PVA hydrogel nanofibers incorporating hyaluronic acid for tissue engineering. *J. Biomater. Nanobiotechnol.* **02**, 353–360 (2011).
43. Akhmetova, A., Myrzakhmetov, B., Wang, Y., Bakenov, Z. & Mentbayeva, A. Development of quaternized chitosan integrated with nanofibrous polyacrylonitrile mat as an anion-exchange membrane. *ACS Omega.* **7**, 45371–45380 (2022).
44. Peng, H. et al. Alkaline polymer electrolyte fuel cells stably working at 80 °C. *J. Power Sources.* **390**, 165–167 (2018).
45. Zeng, L., Zhao, T. S., An, L., Zhao, G. & Yan, X. H. Physicochemical properties of alkaline doped polybenzimidazole membranes for anion exchange membrane fuel cells. *J. Membrane Sci.* **493**, 340–348 (2015).
46. Wang, Y. et al. High performance polymer electrolyte membrane with efficient proton pathway over a wide humidity range and effective cross-linking network. *Reactive Functional Polym.* **161**, 104854 (2021).
47. Brusas, J. R. & Dela Pena, E. M. B. Hygroscopicity of 1:2 choline chloride: ethylene glycol deep eutectic solvent: A hindrance to its electroplating industry adoption. *J. Electrochem. Sci. Technol.* **12**, 387–397 (2021).
48. Li, Y. et al. Development of a crosslinked pore-filling membrane with an extremely low swelling ratio and methanol crossover for direct methanol fuel cells. *Electrochimica Acta.* **232**, 226–235 (2017).
49. Ramesh, S., Shanti, R. & Morris, E. Studies on the plasticization efficiency of deep eutectic solvent in suppressing the crystallinity of corn starch based polymer electrolytes. *Carbohydrate Polym.* **87**, 701–706 (2012).
50. Karas, F., Hnát, J., Paidar, M., Schauer, J. & Bouzek, K. Determination of the ion-exchange capacity of anion-selective membranes. *Int. J. Hydrogen Energy.* **39**, 5054–5062 (2014).
51. Slade, R. & Varcoe, J. Investigations of conductivity in FEP-based radiation-grafted alkaline anion-exchange membranes. *Solid State Ionics.* **176**, 585–597 (2005).
52. Myrzakhmetov, B., Karibayev, M., Wang, Y. & Mentbayeva, A. Density functional theory investigation of intermolecular interactions for hydrogen-bonded deep eutectic solvents. *Eurasian Chemico-Technol. J.* **26**, 29–36 (2024).
53. Wang, G., Weng, Y., Chu, D., Chen, R. & Xie, D. Developing a polysulfone-based alkaline anion exchange membrane for improved ionic conductivity. *J. Membrane Sci.* **332**, 63–68 (2009).
54. Ibrahim, R. K. et al. Physical properties of ethylene glycol-based deep eutectic solvents. *J. Mol. Liquids.* **276**, 794–800 (2019).
55. Taghizadeh, M., Taghizadeh, A., Vatanpour, V., Ganjali, M. R. & Saeb, M. R. Deep eutectic solvents in membrane science and technology: Fundamental, preparation, application, and future perspective. *Separation Purif. Technol.* **258**, 118015 (2021).

Author contributions

A.B. and B.M.: conceptualization, investigation, methodology, visualization, writing-original draft. Y.W. and A.M: conceptualization, supervision, methodology, writing-original draft, writing-review and editing and funding.

Funding

This work was supported by the research grant AP14869880 "Deep eutectic solvent supported polymer-based high performance anion exchange membrane for alkaline fuel cells" project from MES RK.

Declarations

Competing interests

The authors declare no competing interests.

Additional information

Supplementary Information The online version contains supplementary material available at https://doi.org/10.1038/s41598-024-77309-6.

Correspondence and requests for materials should be addressed to A.M.